Geophysical Research Letters

RESEARCH LETTER
10.1029/2022GL097959

Enhanced Photosynthesis and Transpiration in an Old Growth Forest Due To Wildfire Smoke

Bharat Rastogi[1,2,3], Andres Schmidt[1,4], Max Berkelhammer[5], David Noone[6,7], Frederick C. Meinzer[1,8], John Kim[9], and Christopher J. Still[1]

[1]Department of Forest Ecosystems and Society, Oregon State University, Corvallis, OR, USA, [2]Cooperative Institute for Research in the Environmental Sciences, Boulder, CO, USA, [3]Global Monitoring Laboratory, National Oceanic and Atmosphere Administration, Boulder, CO, USA, [4]Department of Fisheries, Wildlife and Conservation Sciences, Oregon State University, Corvallis, OR, USA, [5]Department of Earth and Environmental Sciences, University of Illinois at Chicago, Chicago, IL, USA, [6]College of Earth, Ocean and Atmospheric Sciences, Oregon State University, Corvallis, OR, USA, [7]Department of Physics, University of Auckland, Auckland, New Zealand, [8]Pacific Northwest Research Station, USDA Forest Service, Corvallis, OR, USA, [9]Western Wildland Environmental Threat Assessment Center, USDA Forest Service, Corvallis, OR, USA

Key Points:

- Smoke from a nearby fire warmed and dried the air above an old-growth forest and decreased incoming radiation
- Smoke led to higher canopy photosynthesis and transpiration rates, estimated from eddy covariance and carbonyl sulfide profile measurements, respectively
- These increased fluxes are also facilitated by available deep soil moisture at the site

Supporting Information:

Supporting Information may be found in the online version of this article.

Correspondence to:

B. Rastogi,
bharat.rastogi@colorado.edu

Citation:

Rastogi, B., Schmidt, A., Berkelhammer, M., Noone, D., Meinzer, F. C., Kim, J., & Still, C. J. (2022). Enhanced photosynthesis and transpiration in an old growth forest due to wildfire smoke. *Geophysical Research Letters*, *49*, e2022GL097959. https://doi.org/10.1029/2022GL097959

Received 31 JAN 2022
Accepted 5 MAY 2022

Author Contributions:

Conceptualization: Max Berkelhammer, David Noone, John Kim, Christopher J. Still
Formal analysis: Andres Schmidt, Max Berkelhammer
Methodology: Andres Schmidt, Christopher J. Still
Supervision: David Noone, Christopher J. Still
Writing – review & editing: Andres Schmidt, Max Berkelhammer, David Noone, John Kim, Christopher J. Still

Abstract We document the response of a 2 day wildfire smoke event on a moist temperate coniferous old-growth forest in the western U.S. Wildfire smoke increased air temperature and suppressed relative humidity and total incoming radiation. Despite these conditions a ~10% increase in ecosystem photosynthesis was observed. This was explained by a large increase (41%) in ecosystem-scale stomatal conductance, inferred from measurements of carbonyl sulfide. Increased stomatal conductance contradicts expected stomatal closure at high vapor pressure deficit and was likely caused by an increase in diffuse light and thus shade leaf insolation. Higher ecosystem productivity and transpiration were linked to a greater drawdown of soil moisture. Ecosystem-scale measurements across a diverse range of ecosystems are needed to better understand the canopy response to wildfire smoke, which is an increasingly common phenomenon across large parts of the world, including the forests of western North America.

Plain Language Summary Increases in wildfire intensity have been observed and projected for large parts of western North America, but the impact of smoke from these wildfires on carbon and water fluxes in different ecosystems is not well understood. In this study, we document the response of an old growth coniferous forest located in Pacific Northwestern U.S. to smoke from a nearby wildfire. During this event, the forest experienced warmer, drier and darker conditions. Using measurements of trace gases in the air we observe that the forest canopy increased photosynthesis and transpiration rates. This was due to an increase in scattering of light by smoke particles and facilitated by abundant soil moisture. Increased water-use by trees also reduced the temperature of canopy leaves, potentially preventing them from damaging temperatures. We suggest continued measurements at the ecosystem scale to understand the response of diverse ecosystems to wildfire smoke, an increasingly common phenomenon for large parts of the world, including western North America.

1. Introduction

The enhancement of photosynthesis and terrestrial carbon uptake by diffuse light has been studied in a range of forested ecosystems (e.g., Dowty et al., 2002; Knohl & Baldocchi, 2008; Urban et al., 2007). At the leaf scale, diffuse light is less effective than direct sunlight, leading to lower light use efficiency (LUE) (i.e., the amount of CO_2 fixed per quantum of light; Brodersen et al., 2008). By contrast, at the canopy scale, the less directional nature of diffuse solar radiation leads to less light saturation and photoinhibition and allows a greater proportion of the canopy to be illuminated, thus increasing LUE (Baguskas et al., 2021; Cheng et al., 2015; Hemes et al., 2020) and canopy photosynthesis rates gross primary productivity (GPP), even as incident radiation at the canopy top is reduced (Suyker et al., 2014; Urban et al., 2012). While this enhancement has long been common knowledge in the agriculture community, its impact on global terrestrial carbon cycling gained greater interest after Mt. Pinatubo erupted, changing the global incident radiation budget and leading to enhanced forest carbon uptake (Gu et al., 2003). Subsequently, studies have inferred changes in global carbon sink magnitudes as a function of changing irradiance and temperature (e.g., Li et al., 2018; Zhang et al., 2019), including land-sink

impacts of intentionally increased global aerosol loading (Yang et al., 2020). Cloud cover and aerosol loading from either disturbance (e.g., fire) or anthropogenic emissions typically cause an increase in the diffuse fraction of light. While cloud cover and smoke both usually cause a reduction in total and direct radiation, accompanying variations in environmental conditions can often be different. For instance, cloud cover will usually reduce daytime air temperature and increase relative humidity, while smoke from a nearby fire can cause the opposite weather response. These differences between cool, wet clouds and hot, dry smoke can lead to divergent ecosystem responses to increased diffuse light forcing.

Recently, eddy-flux measurements in North America have been used to show a diffuse light enhancement effect on NEE under mild smoke, and the magnitude of this enhancement has been found to be related to canopy structure, ecosystem-type (e.g., forest vs. bog; McKendry et al., 2019) and photosynthesis type (e.g., ecosystems dominated by C_3 or C_4 crops; Hemes et al., 2020), highlighting the need for additional observations from diverse ecosystems. Measurements of the smoke effect from old-growth forests have not been reported. These forests are structurally different from younger forests and are associated with exceptionally high biomass (Gray et al., 2016) and carbon storage, and substantially increased canopy heterogeneity compared to younger, even-aged plantations and re-growing stands. Moreover, old-growth forests are typically associated with a high leaf area that is distributed over a large canopy volume, allowing for larger absorption of incident radiation (Roberts et al., 2004) and increased carbon accumulation (Stephenson et al., 2014). Such properties allow these forests to maintain higher biodiversity (Franklin, 1981), and increased resilience to climate warming (Frey et al., 2016). However, little is known about how these forests respond to increasingly prevalent wildfire smoke.

Here, we analyze the response of an old-growth moist temperate coniferous forest in the U.S. Pacific Northwest to hot, dry smoke from a nearby fire using measurements of carbon flux from the EC method with simultaneous measurements of carbon monoxide (CO) and carbonyl sulfide (OCS) mixing ratios. CO is used as a tracer for smoke-influence while OCS is used to understand processes that influence ecosystem physiological responses to smoke. OCS is a reduced sulfur gas in the atmosphere which has an uptake pathway from the atmosphere into leaves that is very similar to CO_2 (Berry et al., 2013; Seibt et al., 2010; Stimler et al., 2012; Whelan et al., 2018). Due to the absence of OCS emissions from photosynthesizing leaves and uptake through plant stomata, measurements of OCS have been related to photosynthesis (e.g., Commane et al., 2015; Spielmann et al., 2019) and transpiration (Berkelhammer et al., 2020; Wehr et al., 2017) at canopy scales. We use vertical profiles of OCS mixing ratios to estimate canopy stomatal conductance and transpiration. An independent estimate of canopy stomatal conductance helps explain the GPP response to wildfire smoke and explore possible pathways for smoke to significantly alter GPP and transpiration.

2. Methods

The Rowena fire started on 8 August 2014, just south of the town of Rowena, Oregon, about 50 km east-southeast of the study site (described below). The fire burned for a week, spreading across 2,465 ha of forest. The influence of the fire on the site environment was observed on 10–12 August from in-situ measurements of CO at the site and confirmed using a high-resolution model of atmospheric transport.

2.1. Site Description and Environmental and Carbon Flux Measurements

Measurements were made at the Wind River Experimental Forest, located within the Gifford Pinchot National Forest in southwest Washington state, USA (45°49′13.76″ N; 121°57′06.88″W; 371 m above sea level), about 160 km inland from the Pacific Ocean. The site is well studied and has been described in detail previously (Shaw et al., 2004; Wharton & Falk, 2016; Winner et al., 2004). The forest comprises 478 ha of old-growth evergreen needle-leaf forest, with dominant tree species of Douglas-fir (*Pseudotsuga menziesii*) and Western hemlock (*Tsuga heterophylla*). The tallest Douglas-fir trees are 50–60 m, while shade-tolerant hemlocks are typically between 20 and 50 m high and dominate most of the stem density and above ground biomass (Shaw et al., 2004). Fluxes of CO_2, H_2O and heat, and accompanying environmental variables have been measured on a 70 m tall tower (Falk et al., 2008; Lai et al., 2006; Unsworth et al., 2004; Wharton et al., 2009). The site is part of the Fluxnet network (US-wrc) and fluxes have been reported regularly for the years 1998–2015. NEE was measured using the EC system and gap-filled by identifying a turbulence (friction velocity) threshold (Reichstein et al., 2005). Ecosystem respiration (R_e) was estimated by fitting an empirical relationship between nighttime NEE and air

temperature and moisture, and GPP was calculated as the residual between NEE and R_e. For full data processing protocols, including gap filling, readers are referred to (Wharton & Falk, 2016; Falk et al., 2005, 2008).

2.2. WRF-STILT Runs and Remote Sensing Data Sets

We used the Stochastic Time-Inverted Lagrangian Transport model driven by meteorology from the Weather Research and Forecasting model (STILT; Lin et al., 2003; Nehrkorn et al., 2010) to determine the trajectories of the air masses detected at the measurement location from their source areas during distinct time intervals. WRF-STILT configuration is described in Text S1 of Supporting Information S1.

Aerosol optical depth (AOD) from National Oceanic and Atmsopheric Administration's (NOAA's) Visible Infrared Imaging Radiometer Suite (VIIRS) (Kondragunta et al., 2017) satellite was obtained from NOAA National Centers for Environmental Information (https://www.ncei.noaa.gov/access/metadata/landing-page/bin/iso?id=gov.noaa.ncdc:C01446). Visible Infrared Imaging Radiometer Suite AOD has been extensively used to map smoke (e.g., Hsu et al., 2019; Lee et al., 2018; Lu et al., 2021).

2.3. OCS Flux Estimation

Observations reported here were collected between 7–17 August 2014, as part of a larger measurement campaign (Rastogi, Berkelhammer, Wharton, Whelan, Itter, et al., 2018). Measurements of CO, CO_2, H_2O and OCS mixing ratios are described briefly in Text S2 of Supporting Information S1. Canopy uptake of OCS (F_{OCS} in units of pmol $m^{-2}s^{-1}$) reported here is a subset of values reported previously (Rastogi, Berkelhammer, Wharton, Whelan, Itter, et al., 2018) and was obtained using the following equation (Rastogi, Berkelhammer, Wharton, Whelan, Itter, et al., 2018):

$$F_{\mathrm{OCS}} = -\frac{[\mathrm{OCS}]_{70m} - [\mathrm{OCS}]_{60m}}{R_a^{\mathrm{OCS}}} + S_{\mathrm{OCS}} + F_{\mathrm{OCS,soil}} \quad (1)$$

Where $[OCS]_{70m}$ and $[OCS]_{60m}$ denote mean hourly mixing ratio measurements of OCS at 70 and 60 m above the forest floor and R_a^{OCS} is the aerodynamic resistance to turbulent transport of OCS at the canopy top. A derivation of R_a^{OCS} is shown in Text S2 of Supporting Information S1. S_{OCS} is the change in OCS storage flux (Aubinet et al., 2005), and $F_{OCS,soil}$ is the measured flux of OCS from the forest surface (this includes soil as well as decomposing litter). We did not measure $F_{OCS,soil}$ during this time and use measurements made at the site from similar times in 2015. S_{OCS} accounts for changes in OCS gradients that are not related to surface flux processes, such as entrainment of OCS-enriched air from the Pacific Ocean and mixing of air in the canopy airspace (Rastogi, Berkelhammer, Wharton, Whelan, Itter, et al., 2018). S_{OCS} was calculated using profile measurements located at 70, 60, 10 and 1 m above the forest floor. In a subsequent field campaign (Rastogi, Berkelhammer, Wharton, Whelan, Meinzer, et al., 2018), we installed another sampling line at 20 m above the forest floor, with minimal impacts on S_{OCS}, implying a constant within canopy gradient between 60 and 10 m.

2.4. Estimation of Canopy-Scale Stomatal Conductance, Transpiration and Canopy Temperature

OCS fluxes were used to estimate canopy-scale stomatal conductance to water vapor following Berkelhammer et al. (2020) and Wehr et al. (2017). First, total conductance to OCS $\left(g_t^{OCS}\right)$ was estimated by normalizing F_{OCS} by ambient OCS mixing ratios. g_t^{OCS} is akin to a depositional velocity. This ensures that stomatal conductance as inferred by F_{OCS} is minimally impacted by elevated OCS mixing ratios (e.g., Kooijmans et al., 2021).

$$g_t^{\mathrm{OCS}} = -\frac{F_{\mathrm{OCS}}}{[\mathrm{OCS}]_{70m}} \quad (2)$$

g_t^{OCS} comprises boundary layer conductance to OCS (g_b^{OCS}), stomatal conductance (g_s^{OCS}) and mesophyll conductance (g_m^{OCS}). All conductances are reported in [mol $m^{-2}s^{-1}$].

$$g_t^{\mathrm{OCS}} = \left[\frac{1}{g_b^{\mathrm{OCS}}} + \frac{1}{g_s^{\mathrm{OCS}}} + \frac{1}{g_m^{\mathrm{OCS}}}\right]^{-1} \quad (3)$$

Conductances are described in Text S4 of Supporting Information S1. g_s^{OCS} is converted to $g_s^{H_2O}$ by multiplying by 1.94 (to account for the ratio of diffusivities of OCS and H_2O in air- Seibt et al., 2010). An uncertainty analyses on $g_s^{H_2O}$ based on component terms is provided in Text S4 of Supporting Information S1. Specifically, we tested the impact of different semi-empirical models of aerodynamic resistance (Equation 1) and mesophyll conductance on modeled $g_s^{H_2O}$. $g_s^{H_2O}$ is further used to infer canopy transpiration following Jarvis and Mcnaughton (1986), Martin (1989) and Martin et al. (1999), described in Text S3 of Supporting Information S1. Along with error propagation based on the uncertainty analyses (Text S4 of Supporting Information S1).

We estimated canopy temperature, $T_{LW\uparrow}$ from measured upwelling longwave radiation as (Norman & Becker, 1995):

$$T_{LW_\uparrow} = \left(\frac{LW_\uparrow}{\alpha_{IR}\sigma}\right)^{1/4} \quad (4)$$

Still et al. (2021) show that this metric of canopy temperature is highly correlated with measurements of canopy temperatures using a thermal camera at the site (slope = 0.96; correlation coefficient = 0.99).

Canopy LUE was calculated as the ratio of GPP to absorbed Photosynthetically Active Radiation (APAR- estimated following Bonan, 2015) as:

$$\text{APAR} = \text{PAR}.\, e^{-K.LAI} \quad (5)$$

Where PAR was measured above canopy, K is the light extinction coefficient (assumed daytime mean value of 0.5), and LAI is one-sided leaf area index.

3. Results and Discussion

3.1. Smoke and Other Meteorological Conditions

Calculated daily footprints of the tower (represented by the blue dot) from WRF-STILT at 70 m from 9 August to 12 August are shown in Figure S1a–S1d in Supporting Information S1. Rowena is located southeast of the site (red patch in southwest corner in Figure S1a–S1d in Supporting Information S1). On 10 and 11 August, the air at the tower was directly influenced by the fire (Figure S1b–S1c in Supporting Information S1), corresponding to increases in gas mixing ratios (discussed in Section 3.2). Here, we show daytime mean values, where we define daytime as periods when incoming PAR exceeds 100 [μmol $m^{-2}s^{-1}$]. Mean daytime values for 7–17 August are shown in Figure 1 and hourly timeseries' of environmental responses are shown in Figure S3 of Supporting Information S1. Environmental conditions before the smoke event (7–9 August) are characterized by generally sunny and warm days (Shaw et al., 2004). Mean daytime temperature during those days was ~23 [°C] (Figure 1a) and the mean minimum temperature was ~13 [°C] (Figure S3a in Supporting Information S1). During the smoke event, daytime maximum temperatures soared to ~35 [°C], minimum temperatures stayed high at ~19.5 [°C] (Figure S3a in Supporting Information S1), relative humidity declined from ~50% on 8 August to below 23% on 11 August (Figure 1b). A large increase in daytime vapor pressure deficit (VPD) from ~2 [kPa] to exceeding four [kPa], was also observed on smoke-affected days (left axis in Figure 1b). Turbulence, as inferred by measurement of friction velocity (u_*; right axis in Figure 1b) also decreased on 9 August, stayed low during the smoke event, varied as sky conditions changed from smoke to overcast, but was higher than the critical threshold at the site (0.3 ms^{-1}; Falk et al., 2008), except on 15 August. A decrease in incoming short-wave radiation ($SW_\downarrow$) was observed on 10 and 11 August (mean daytime $SW_\downarrow$ declined from 580 [Wm^{-2}] on 9 August to 308 [Wm^{-2}] on 11 August; Figure 1c), and mean daytime incoming PAR and net radiation declined by ~16–18% (red squares and green triangles in Figure 1c). On 12 August, mean daytime PAR was ~700 [μmol $m^{-2}s^{-1}$], daytime air temperature decreased from 31.1 [°C] the day before to 22.8 [°C], and relative humidity increased from 26% to 64%. This resulted in a large reduction in mean daytime peak VPD (from >4 on 11 August to 1 [kPa] on 12 August; Figure 1c). The decrease in PAR and $SW_\downarrow$ was accompanied by a concomitant increase in incoming longwave radiation ($LW_\downarrow$; Figure S3d in Supporting Information S1). This was due to widespread cloud cover, leading eventually to 1.65 mm of rain between 2 and 10 p.m. (Figure S3a in Supporting Information S1). Overcast conditions due to cloud cover persisted through 15 August. Cloud cover dissipated on 16 and 17 August and sky conditions were clear, with some haziness due to smoke from distant fires in Washington and British Columbia, Canada (see

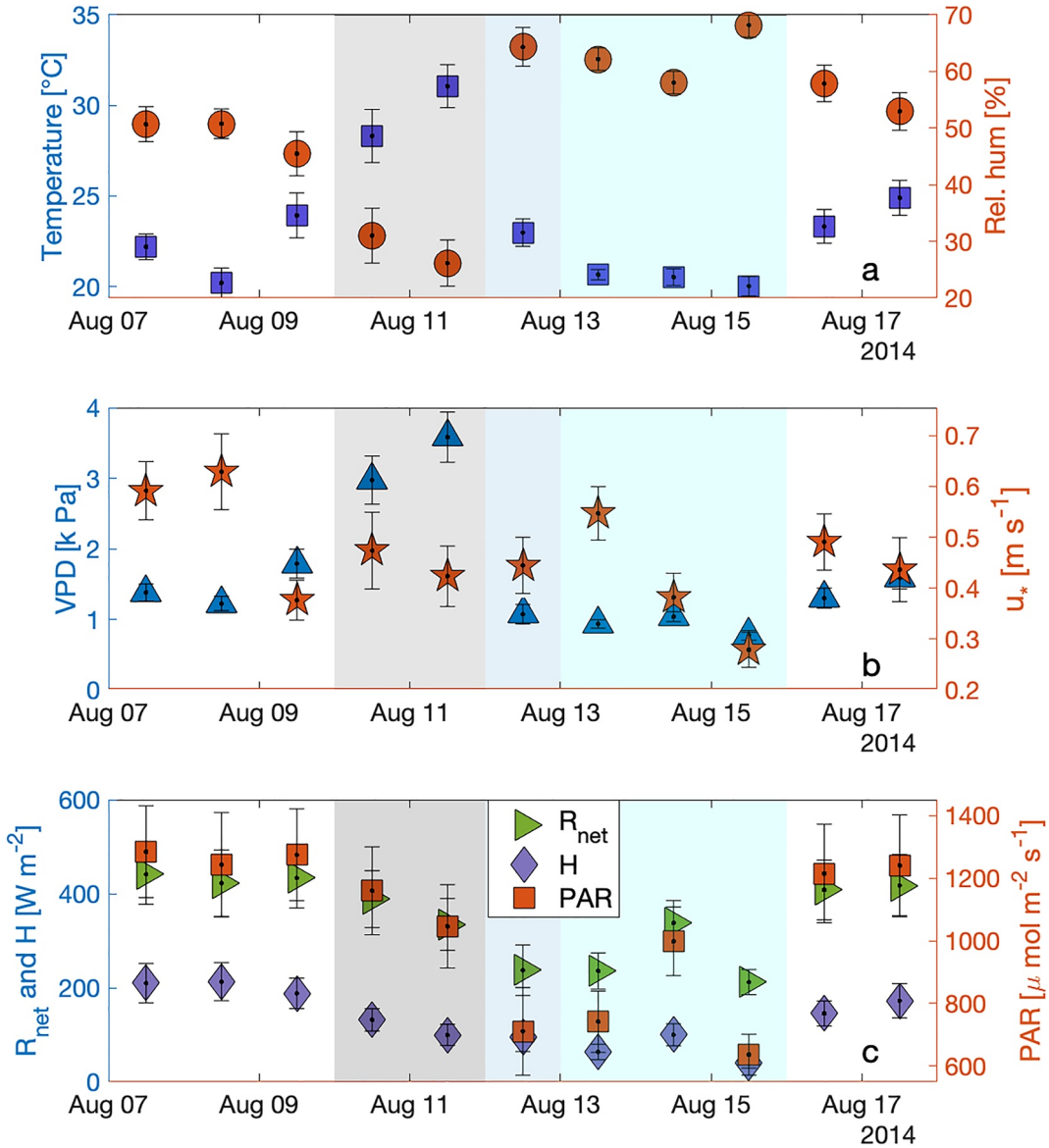

Figure 1. Environmental conditions during the 10 day period that includes the smoke event (shaded in gray). On 12 August the site experienced widespread overcast conditions and rain (shaded in blue). Cloud cover persisted between 13 and 15 August (shaded in cyan). Error bars indicate the standard error around the mean for each quantity.

slight increase in CO mixing ratios in Figure 2a). Patterns of sensible heat flux (purple diamonds in Figure 1c) generally followed net radiation (Figure 1c).

3.2. Profile Measurements

Profiles of CO show a steady increase starting on 10 August, peaking around midday on 12 August (Figure 2a). Combined with AOD data from VIIRS (right axis in Figure 2a), these indicate that the site experienced smoke during these days. CO peaked in the evening on 11 August and at 1 p.m. on 12 August (increasing from ~100 [ppb] between 7–9 August to ~230 [ppb] on 11 and 12 August), declining sharply thereafter. An increase was measured in CO_2 mixing ratios, most prominently in the understory (yellow line in Figure 2b consequence of enhanced soil and understory plant respiration (Figure 3a) due to higher temperatures (Figure S4 in Supporting Information S1) and topographically generated sub-canopy airflows (Paw U et al., 2004). H_2O mixing ratios and relative humidity decreased during 10–11 August, indicating that the canopy air was drier. Profiles of OCS show

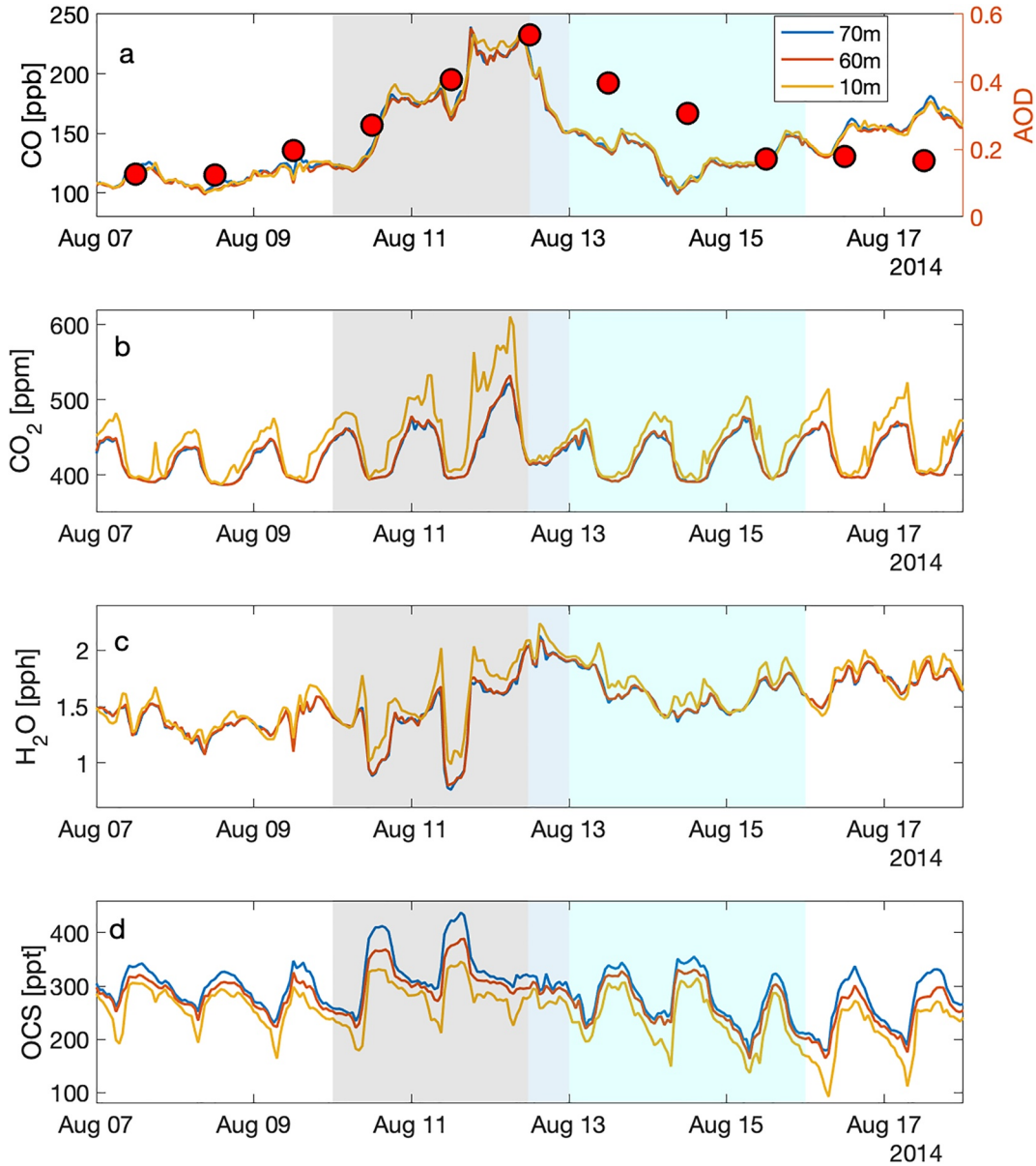

Figure 2. Mixing ratios of gases measured at the site (left *y*-axis in panels (a–d)) and aerosol optical depth (AOD - right axis) from National Oceanic and Atmsopheric Administration's Visible Infrared Imaging Radiometer Suite (solid circles in (a)). Gray shading denotes days that were influenced by smoke, blue shading shows influence of clouds and light rain, and cyan shading shows influence of cloud cover. Colors indicate height above the forest surface. The canopy height is 60 m and the leaf area profile is shown in Figure S1e of Supporting Information S1.

a sharp increase starting 10 August. Mid-day maximum [OCS] above the canopy (70 m; blue line in Figure 2d) increased from ~325 [ppt] on 8 and 9 August to >400 [ppt] on 10 and 11 August. This increase was persistent all the way to the understory as [OCS] at 10 m (yellow curve in Figure 2d) increased from ~285 [ppt] on 8–9 August to ~323 [ppt] on 10 and 11 August . On 12 August, CO, CO_2, AOD and H_2O all remained high until midday, but OCS mixing ratios above the canopy and in-canopy gradients (Figure S5 in Supporting Information S1) were reduced. This was driven by a lack of entrainment of free tropospheric air into the canopy airspace. Daytime increases in canopy OCS at the site occur primarily through entrainment (Rastogi, Berkelhammer, Wharton, Whelan, Itter, et al., 2018), a phenomenon that was limited during this time as cloud cover, rainfall and low wind speeds prevented the entrainment of OCS-enriched air from the upper atmosphere. Overcast conditions persisted on 13 August; consequently, relative humidity and H_2O mixing ratios remained high. However, greater mixing

of canopy air with air aloft (Figures 1b, S3e in Supporting Information S1) facilitated entrainment of free tropospheric OCS in the canopy and venting of trapped CO and CO_2 on that day.

3.3. Impact on Ecosystem Fluxes

Long-term measurements of daytime mean NEE at the site reveal that the site is usually near-neutral with respect to CO_2 exchange with the atmosphere during this time of year (Wharton & Falk, 2016). Mean daytime CO_2 sink (NEE) decreased slightly from -2.97 ± 0.36 [μmol $m^{-2}s^{-1}$] between 7 and 9 August to -2.00 [μmol $m^{-2}s^{-1}$] on 11 August). The ecosystem was a net source of carbon on 12 and 15 August (Figure 3a). Ecosystem respiration estimated from NEE measurements (upward facing yellow triangles in Figure 3a) closely followed air temperature, as expected. We inferred a 10% increase in mean daytime GPP during the smoke event (green triangles in Figure 3a). GPP was highest during the smoke event, declining thereafter due to light limitation from overcast sky conditions. On 14 August, the light limitation is relieved (PAR increases from 750 to 1,050 [μmol $m^{-2}s^{-1}$], but this day is characterized by low turbulence until mid-afternoon (right axis in Figure 1b; hourly values shown in Figure S3e in Supporting Information S1). GPP remains low on 15 August when PAR (Figure 1c) and turbulence (Figure 1b) are both suppressed due to widespread cloud cover.

We tested two other commonly used models for CO_2 flux-partitioning at the site. These models are based on the Reichstein et al., 2005 and Lasslop et al., 2010 algorithms, and are available online by the Max-Planck Insitüt for Biogeochemistry (https://www.bgc-jena.mpg.de/bgi/index.php/Services/REddyProcWeb). The Reichstein model yielded a similar increase in GPP during the smoke-days. This is unsurprising as the site-specific flux partitioning model used here is based in part on the Reichstein model, but with modifications to incorporate a soil moisture feedback on respiration (Falk et al., 2008). The Lasslop method showed the opposite response, that is, a decrease in GPP during the smoke-event (Figure S6a in Supporting Information S1). However, we find that during the smoke event, respiration fluxes estimated in that model decreased even though a substantial increase in air temperature is observed (Figures 1a, S6b in Supporting Information S1). We find this unrealistic and therefore disregard the Lasso model result. The decrease in respiration in that model is likely caused by an over-estimated VPD-induced negative feedback on GPP (Lasslop et al., 2010).

We observed a large (68%) increase in ecosystem uptake of OCS during the smoke event (daytime mean F_{OCS} increased from -28.67 ± 2.52 to -48.24 ± 3.72 [pmol $m^{-2}s^{-1}$]; Figure 3b). Friction velocity measurements (Figure 1b and S3e in Supporting Information S1) suggest that mechanically induced vertical exchange was well developed during the 2-day period when concentrations of OCS at the tower were influenced by the Rowena fire emissions (10–11 August, Figures 2 & S1 in Supporting Information S1). While we could not assess changes in horizontal advection during the smoke event, detailed investigations of horizontal advection at the site (Falk et al., 2008; Park & Paw U, 2004; Paw U et al., 2004) have revealed that its effect on total flux is negligible under unstable conditions (when $u_* \geq 0.3$ ms^{-1}). Hence, while some effect of advective transport on the OCS fluxes must be assumed when interpreting the results, vertical turbulent exchange remains the dominant component of OCS fluxes reported here. Canopy-scale stomatal conductance to water vapor ($g_s^{H_2O}$), inferred from OCS uptake (Equations 1–3, Text S3 in Supporting Information S1), increased by 41% from 0.22 ± 0.01 to 0.31 ± 0.02 [mol $m^{-2}s^{-1}$] (Figure 3c). This is surprising since above-canopy VPD also increased on 10 and 11 August (Figure 3b) and therefore contradicts expected leaf-level stomatal closure under elevated VPD (Novick et al., 2016; Oren et al., 1999). However, the increase in canopy-scale $g_s^{H_2O}$ resulted from leaf responses integrated across the entire canopy and would explain the GPP enhancement (Figure 3a), even as incoming PAR decreased (Figure 1c).

Along with elevated VPD, increased $g_s^{H_2O}$ caused an increase in modeled canopy transpiration (Figure 3c). During most of this time period, we were unable to measure H_2O vapor fluxes using the EC instrument. Due to a sensor error, these values were negative during the week of 7–14 August (blue squares in Figure S7 of Supporting Information S1). However, during the full extent of the observation campaign (Rastogi, Berkelhammer, Wharton, Whelan, Itter, et al., 2018), OCS-based transpiration was positively correlated with eddy-flux based evapotranspiration (ET) fluxes (Figure S7 in Supporting Information S1). H_2O flux measurements were available between August (pink squares in Figure 3c) and show higher values compared to OCS-based transpiration estimates. This is due to non-transpiration components of the ET flux, specifically the additional evaporation of water droplets intercepted by the canopy after rain fell on 12 August. Both OCS-based transpiration and EC-based ET increase

on 16–17 August when cloud cover dissipated, and the sky was mostly clear (Figures 1c and S3d in Supporting Information S1).

One confirmation of higher modeled transpiration rates is the cooling of canopy temperatures as inferred from measured upwelling longwave radiation. While canopy temperatures remained higher than air temperature, increased transpiration reduced the difference between air and canopy temperatures, possibly preventing damage to leaves from elevated air temperatures during the smoke event (Figure 3d; a time series of the difference in inferred canopy and measured air temperatures is shown in Figure S8 in Supporting Information S1). Increased transpiration rates may also have been driven by increased longwave downwelling ($LW_{\downarrow}$) radiation during those days (Figure S9a in Supporting Information S1). $LW_{\downarrow}$ was also high between 12 and 16 August due to highly overcast conditions.

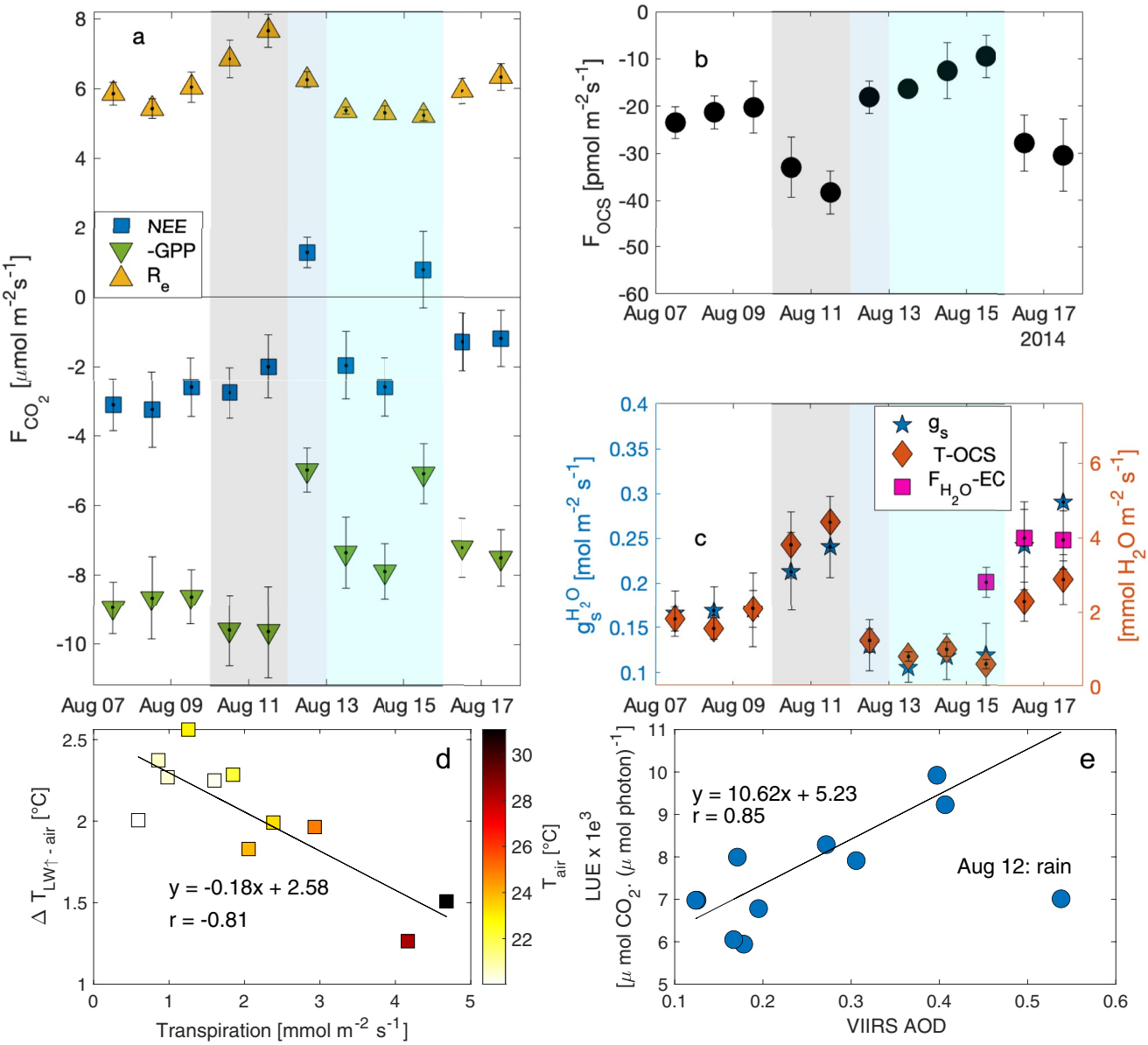

Figure 3. CO_2 fluxes (a), canopy carbonyl sulfide flux (b), modeled canopy stomatal conductance and water fluxes (c). Modeled transpiration plotted against the difference between canopy and air temperatures (d), and light use efficiency plotted against Visible Infrared Imaging Radiometer Suite Aerosol optical depth (AOD) (e). The site experienced rainfall on 12 August, and this point is excluded from the regression shown in (e). Data plotted in each panel represent daytime means (where daytime is defined when PAR exceeds 100 [μ mol m^{-2}s^{1}]. Areas shaded in gray and blue indicate smoky and cloudy/rainy conditions respectively. Error bars indicate the standard error around the mean for each plotted quantity.

The perplexing increase in modeled canopy-scale stomatal conductance is likely explained by enhanced diffuse light from smoke. An increase in diffuse light would therefore have illuminated a greater fraction of the heterogenous canopy and allowed more leaves lower in the canopy (Figure S1e in Supporting Information S1) to assimilate carbon and transpire. Canopy light use efficiency (LUE) was strongly correlated with satellite derived AOD (Figure 3e), except on 12 August when the site experienced overcast conditions and rainfall. We expect LUE to decrease when PAR is highly suppressed but exclude this point from the regression line (shown in Figure 3e) since more data would be needed to determine the inflection point in the relationship between AOD and LUE at the site. We did not measure diffuse light or spectral changes in incoming light due to smoke and cloud-cover. However, aerosols that comprise smoke particles are expected to enhance the diffuse fraction of available PAR (Cohan et al., 2002). The ratio of PAR to incoming shortwave radiation was variable during this time (Figure S9b in Supporting Information S1). This ratio was lowest on 10 August (smoke) and highest during overcast conditions (12–15 August), indicating that fewer total photons normalized to incoming radiation were available for photosynthesis (McKendry et al., 2019) under smoky conditions. The ratio increased under cloudy conditions, but GPP was limited by total available PAR between 12 and 16 August (Figure 1c). The increase in LUE despite a slight decrease in this ratio during the smoke-event also suggests that the proportion of illuminated leaves must have increased during these days. Diffuse light measurements were made at the site in 2015 and positively correlated to LUE (Figure S9c in Supporting Information S1; data from Rastogi, Berkelhammer, Wharton, Whelan, Meinzer, et al., 2018).

Higher GPP during the smoke-event was facilitated by relatively high soil moisture at the site. Continuous soil moisture measurements made at 30 cm depth between 2007 and 15 show that soil moisture for the month of August was highest in 2014 (Figure S10a in Supporting Information S1). Mean daytime GPP between 7 and 17 August was correlated with the measured daily drawdown of soil moisture at various depths between 20 and 150 cm below the forest surface (drawdown is defined as the difference between maximum and minimum soil moisture for each day; Figure S10b in Supporting Information S1). Large trees at the site that dominate the carbon-water exchange with the atmosphere (Harmon et al., 2004) have deep roots and can access soil water even during prolonged summer drought as rates of soil drying are relatively low, despite high frictional resistance encountered by leaves in the tall canopy (Brooks et al., 2006; Meinzer et al., 2006; Warren et al., 2005).

4. Conclusions

We analyzed the impact of hot, dry smoke from a nearby fire (~50 km away) on ecosystem functioning of a moist temperate old-growth forest in the U.S. Pacific Northwest. During the smoke-event we measured a doubling of CO mixing ratios, increased CO_2 mixing ratios and an increase in OCS mixing ratios. Smoke-induced increases in aerosol loading (observed via satellite retrievals of AOD) led to a reduction in incoming solar radiation, increased air temperatures by ~8 [°C] and reduced daytime relative humidity by ~40%, increasing mean daytime VPD from 1 [kPa] to >4 [kPa]. Even as temperature and VPD increased, a ~10% increase in GPP (estimated from NEE measurements) was observed. Using established methods for inferring canopy-scale stomatal conductance from measured gradients of OCS and a big-leaf model of conductances, we find that increased canopy stomatal conductance explains the GPP enhancement. While stomata of individual needles, especially at the canopy top, would have mostly closed at high VPD, enhanced diffuse light during the smoke-event likely illuminated leaves lower in the canopy, increasing stomatal conductance of those leaves as well as canopy light-use efficiency. The bulk of the leaf area at the site is located ~30–40 m below the tops of the tallest trees, and remains shaded when incident radiation is direct, likely received increased light, enabling photosynthesis and increasing the old-growth forest's resilience to elevated temperature and VPD during the smoke-event.

A strong enhancement of GPP and LUE due to increased diffuse light from cool, wet clouds been observed previously, including at this site (Figure S9c in Supporting Information S1; Rastogi, Berkelhammer, Wharton, Whelan, Meinzer, et al., 2018; Wharton & Falk, 2016) but the effect of hot, dry smoke from a nearby fire has not been studied here or in similar forests. While the enhancement of diffuse light is similar for partly cloudy and smoky conditions (when total incoming light is not highly suppressed), other environmental conditions are quite different. Notably, summertime cloud cover cools and moistens the air, relieving VPD constraints on stomatal conductance and photosynthesis. During the smoke event, canopy air warmed and dried, leading to an increase in the atmospheric demand for moisture from canopy leaves. Thus, we conclude that the diffuse light enhancement

of photosynthesis at the site was independent of VPD impacts on stomatal conductance. During these hot, dry and smoky days, soil water uptake by the forest increased as a result of higher transpiration rates, leading to partial cooling of the canopy temperatures.

Old-growth forests contain some of the largest and most vulnerable stores of carbon (Harris et al., 2021; Lutz et al., 2018; Luyssaert et al., 2008; Pan et al., 2011) and are increasingly under the influence of fire-smoke from boreal (Walker et al., 2019) to tropical regions (Gatti et al., 2021). Climate change is expected to alter fire regimes (Halofsky et al., 2020; Parks et al., 2018), for for example, in the Western U.S., increases in fire frequency have been observed and linked to increased aridity (Abatzoglou & Williams, 2016; Holden et al., 2018; LeRoy Westerling, 2016). Increases in drought frequency and reductions in soil moisture have been predicted and observed for the region (Cartwright et al., 2020; Peltier & Ogle, 2019; Strzepek et al., 2010; Xu et al., 2019). Additionally, declines in coastal summertime low cloud frequency have also been observed (Dye et al., 2020), exacerbating growing season forest moisture stress. Ecosystem productivity and water-use efficiency are both highly sensitive to VPD and soil moisture at the site (Jiang et al., 2019; Wharton & Falk, 2016), and for forests in much of the western U.S. (Berner et al., 2017). Therefore, the increase in GPP via increased conductance and LUE as a response to smoke, may only be sustained while these trees have access to enough sub-surface water to counter the impact of rising temperature and VPD.

The many ways that smoke impacts ecosystem productivity and carbon cycle need to be understood more comprehensively. For instance, little is known about how ecosystem carbon and water cycling respond to factors such as increasing fire-season lengths, the interacting effects of diffuse light enhancement and water-stress, or the effect of long-range transported smoke compared to that from a nearby fire. Smoke can also impact canopy chemistry by potentially increasing ambient ozone mixing ratios, which can reduce GPP via negative impacts on $g_s^{H_2O}$. (e.g., Hemes et al., 2020; Yue & Unger, 2018) Additionally, black and brown smoke particles can possibly alter the spectral qualities of incoming light differently from water molecules that comprise clouds. We suggest future studies consider the impacts of ozone and smoke particles on stomatal conductance, GPP and LUE. Continued ecosystem-scale measurements can help in understanding the fate of these ecosystems under an evolving warmer, drier, and smokier climate.

Data Availability Statement

Data used in this study are archived at https://doi.org/10.5281/zenodo.6555248. These data are a subset of measurements reported in Rastogi, Berkelhammer, Wharton, Whelan, Itter, et al. (2018). For further information readers are referred to that study. Long term eddy flux data for Wind River are available at https://doi.org/10.17190/AMF/1246114.

Acknowledgments
We would like to thank the U.S. Forest Service and the University of Washington for letting us use the research facility at Wind River. In particular, we thank Dr. Ken Bible and Matt Schroeder for experiment setup and maintenance throughout the measurement campaign. This research was funded by Joint venture agreement 14-JV-1126191952-095 between the USDA Forest Service and Oregon State University.

References

Abatzoglou, J. T., & Williams, A. P. (2016). Impact of anthropogenic climate change on wildfire across western US forests. *Proceedings of the National Academy of Sciences*, *113*(42), 11770–11775. https://doi.org/10.1073/pnas.1607171113

Aubinet, M., Berbigier, P., Bernhofer, C., Cescatti, A., Feigenwinter, C., Granier, A., et al. (2005). Comparing CO_2 storage and advection conditions at night at different carboeuroflux sites. *Boundary-Layer Meteorology*, *116*(1), 63–94. https://doi.org/10.1007/s10546-004-7091-8

Baguskas, S. A., Oliphant, A. J., Clemesha, R. E. S., & Loik, M. E. (2021). Water and light-use efficiency are enhanced under summer coastal fog in a California agricultural system. *Journal of Geophysical Research: Biogeosciences*, *126*, 1–16. https://doi.org/10.1029/2020JG006193

Berkelhammer, M., Alsip, B., Matamala, R., Cook, D., Whelan, M. E., Joo, E., et al. (2020). Seasonal evolution of canopy stomatal conductance for a prairie and maize field in the Midwestern United States from continuous carbonyl sulfide fluxes. *Geophysical Research Letters*, *47*(6). https://doi.org/10.1029/2019GL085652

Berner, L. T., Law, B. E., & Hudiburg, T. W. (2017). Water availability limits tree productivity, carbon stocks, and carbon residence time in mature forests across the western US. *Biogeosciences*, *14*(2), 365–378. https://doi.org/10.5194/bg-14-365-2017

Berry, J., Wolf, A., Campbell, J. E., Baker, I., Blake, N., Blake, D., et al. (2013). A coupled model of the global cycles of carbonyl sulfide and CO_2: A possible new window on the carbon cycle. *Journal of Geophysical Research: Biogeosciences*, *118*, 842–852. https://doi.org/10.1002/jgrg.20068

Bonan, G. (2015). *Ecological climatology: Concepts and applications*. Cambridge University Press.

Brodersen, C. R., Vogelmann, T. C., Williams, W. E., & Gorton, H. L. (2008). A new paradigm in leaf-level photosynthesis: Direct and diffuse lights are not equal. *Plant, Cell and Environment*, *31*(0), 159–164. https://doi.org/10.1111/j.1365-3040.2007.01751.x

Brooks, J. R., Meinzer, F. C., Warren, J. M., Domec, J. C., & Coulombe, R. (2006). Hydraulic redistribution in a Douglas-fir forest: Lessons from system manipulations. *Plant, Cell and Environment*, *29*(1), 138–150. https://doi.org/10.1111/j.1365-3040.2005.01409.x

Cartwright, J. M., Littlefield, C. E., Michalak, J. L., Lawler, J. J., & Dobrowski, S. Z. (2020). Topographic, soil, and climate drivers of drought sensitivity in forests and shrublands of the Pacific Northwest, USA. *Scientific Reports*, *10*, 1–13. https://doi.org/10.1038/s41598-020-75273-5

Cheng, S. J., Bohrer, G., Steiner, A. L., Hollinger, D. Y., Suyker, A., Phillips, R. P., & Nadelhoffer, K. J. (2015). Variations in the influence of diffuse light on gross primary productivity in temperate ecosystems. *Agricultural and Forest Meteorology*, *201*, 98–110. https://doi.org/10.1016/j.agrformet.2014.11.002

Cohan, D. S., Xu, J., Greenwald, R., Bergin, M. H., & Chameides, W. L. (2002). Impact of atmospheric aerosol light scattering and absorption on terrestrial net primary productivity. *Global Biogeochemical Cycles*, *16*(4), 37–1–37–12. https://doi.org/10.1029/2001gb001441

Commane, R., Meredith, L. K., Baker, I. T., Berry, J. A., Munger, J. W., Montzka, S. A., et al. (2015). Seasonal fluxes of carbonyl sulfide in a midlatitude forest. *Proceedings of the National Academy of Sciences*, *112*(46), 14162–14167. https://doi.org/10.1073/pnas.1504131112

Dowty, P. R., Verma, S. B., Black, T. A., Falge, E. M., Vesala, T., Baldocchi, D., & Gu, L. (2002). Advantages of diffuse radiation for terrestrial ecosystem productivity. *Journal of Geophysical Research*, *107*, 2–23. https://doi.org/10.1029/2001jd001242

Dye, A. W., Rastogi, B., Clemesha, R. E. S., Kim, J. B., Samelson, R. M., Still, C. J., & Williams, A. P. (2020). Spatial patterns and trends of summertime low cloudiness for the Pacific Northwest, 1996–2017. *Geophysical Research Letters*, *47*(16). https://doi.org/10.1029/2020GL088121

Falk, M., Paw U, K. T., Wharton, S., & Schroeder, M. (2005). Is soil respiration a major contributor to the carbon budget within a Pacific Northwest old-growth forest? *Agricultural and Forest Meteorology*, *135*(1–4), 269–283. https://doi.org/10.1016/j.agrformet.2005.12.005

Falk, M., Wharton, S., Schroeder, M., Ustin, S., & U, K. T. P. (2008). Flux partitioning in an old-growth forest: Seasonal and interannual dynamics. *Tree Physiology*, *28*(4), 509–520. https://doi.org/10.1093/treephys/28.4.509

Franklin, J. F. (1981). *Ecological characteristics of old-growth Douglas-fir forests*. US Department of Agriculture, Forest Service.

Frey, S. J. K., Hadley, A. S., Johnson, S. L., Schulze, M., Jones, J. A., & Betts, M. G. (2016). Spatial models reveal the microclimatic buffering capacity of old-growth forests. *Science Advances*, *2*(4), e1501392. https://doi.org/10.1126/sciadv.1501392

Gatti, L. V., Basso, L. S., Miller, J. B., Gloor, M., Gatti Domingues, L., Cassol, H. L. G., et al. (2021). Amazonia as a carbon source linked to deforestation and climate change. *Nature*, *595*(7867), 388–393. https://doi.org/10.1038/s41586-021-03629-6

Gray, A. N., Whittier, T. R., & Harmon, M. E. (2016). Carbon stocks and accumulation rates in Pacific Northwest forests: Role of stand age, plant community, and productivity. *Ecosphere*, *7*(1). https://doi.org/10.1002/ecs2.1224

Gu, L., Baldocchi, D. D., Wofsy, S. C., William Munger, J., Michalsky, J. J., Urbanski, S. P., & Boden, T. A. (2003). Response of a deciduous forest to the Mount Pinatubo eruption: Enhanced photosynthesis. *Science*, *299*(5615), 2035–2038. https://doi.org/10.1126/science.1078366

Halofsky, J. E., Peterson, D. L., & Harvey, B. J. (2020). *Changing wildfire, changing forests: The effects of climate change on fire regimes and vegetation in the Pacific Northwest*.

Harmon, M., Bible, K., Ryan, M., Shaw, D., Chen, H., Klopatek, J., & Li, X. (2004). Production, respiration, and overall carbon balance in an old-growth pseudotsuga-tsuga forest ecosystem. *Ecosystems*, 498–512. https://doi.org/10.1007/s10021-004-0140-9

Harris, N. L., Gibbs, D. A., Baccini, A., Birdsey, R. A., de Bruin, S., Farina, M., et al. (2021). Global maps of twenty-first century forest carbon fluxes. *Nature Climate Change*, *11*(3), 234–240. https://doi.org/10.1038/s41558-020-00976-6

Hemes, K. S., Verfaillie, J., & Baldocchi, D. D. (2020). Wildfire-smoke aerosols lead to increased light use efficiency among agricultural and restored wetland land uses in California's central valley. *Journal of Geophysical Research: Biogeosciences*, *125*(2), e2019JG005380. https://doi.org/10.1029/2019JG005380

Holden, Z. A., Swanson, A., Luce, C. H., Jolly, W. M., Maneta, M., Oyler, J. W., et al. (2018). Decreasing fire season precipitation increased recent western US forest wildfire activity. *Proceedings of the National Academy of Sciences of the United States of America*, *115*(36), E8349–E8357. https://doi.org/10.1073/pnas.1802316115

Hsu, N. C., Lee, J., Sayer, A. M., Kim, W., Bettenhausen, C., & Tsay, S. C. (2019). VIIRS deep blue aerosol products over land: Extending the EOS long-term aerosol data records. *Journal of Geophysical Research: Atmospheres*, *124*, 4026–4053. https://doi.org/10.1029/2018JD029688

Jarvis, P. G., & Mcnaughton, K. G. (1986). Stomatal control of transpiration: Scaling up from leaf to region. *Advances in Ecological Research*, *15*, 1–49. https://doi.org/10.1016/S0065-2504(08)60119-1

Jiang, Y., Still, C. J., Rastogi, B., Page, G. F. M., Wharton, S., Meinzer, F. C., et al. (2019). Trends and controls on water-use efficiency of an old-growth coniferous forest in the Pacific Northwest. *Environmental Research Letters*, *14*(7), 074029. https://doi.org/10.1088/1748-9326/ab2612

Knohl, A., & Baldocchi, D. D. (2008). Effects of diffuse radiation on canopy gas exchange processes in a forest ecosystem. *Journal of Geophysical Research*, *113*(G2), 1–17. https://doi.org/10.1029/2007JG000663

Kondragunta, S., Laszlo, I., Ciren, P., Zhang, H., Liu, H., Huang, J., & Huff, A. (2017). Exceptional events monitoring using S-NPP VIIRS aerosol products. *IEEE international geoscience and remote sensing symposium (IGARSS)* (pp. 1285–1287). IEEE.

Kooijmans, L. M., Cho, A., Ma, J., Kaushik, A., Haynes, K. D., Baker, I., et al. (2021). Evaluation of carbonyl sulfide biosphere exchange in the Simple Biosphere Model (SiB4). *Biogeosciences*, *18*(24), 6547–6565. https://doi.org/10.5194/bg-18-6547-2021

Lai, C., Ehleringer, J. R., Bond, B. J., & PAW U, K. T. (2006). Contributions of evaporation, isotopic non-steady state transpiration and atmospheric mixing on the $\delta^{18}O$ of water vapour in Pacific Northwest coniferous forests. *Plant, Cell and Environment*, *29*(1), 77–94. https://doi.org/10.1111/j.1365-3040.2005.01402.x

Lasslop, G., Reichstein, M., Papale, D., Richardson, A., Arneth, A., Barr, A., et al. (2010). Separation of net ecosystem exchange into assimilation and respiration using a light response curve approach: Critical issues and global evaluation. *Global Change Biology*, *16*(1), 187–208. https://doi.org/10.1111/j.1365-2486.2009.02041.x

Lee, M. S., Hollinger, D. Y., Keenan, T. F., Ouimette, A. P., Ollinger, S. V., & Richardson, A. D. (2018). Model-based analysis of the impact of diffuse radiation on CO_2 exchange in a temperate deciduous forest. *Agricultural and Forest Meteorology*, *249*, 377–389. https://doi.org/10.1016/j.agrformet.2017.11.016

LeRoy Westerling, A. (2016). Increasing western US forest wildfire activity: Sensitivity to changes in the timing of spring. *Philosophical Transactions of the Royal Society B: Biological Sciences*, *371*(1696), 20150178. https://doi.org/10.1098/rstb.2015.0178

Li, W., Ciais, P., Wang, Y., Yin, Y., Peng, S., Zhu, Z., et al. (2018). Recent changes in global photosynthesis and terrestrial ecosystem respiration constrained from multiple observations. *Geophysical Research Letters*, *45*(2), 1058–1068. https://doi.org/10.1002/2017GL076622

Lin, J. C., Gerbig, C., Wofsy, S. C., Andrews, A. E., Daube, B. C., Davis, K. J., & Grainger, C. A. (2003). A near-field tool for simulating the upstream influence of atmospheric observations: The Stochastic Time-Inverted Lagrangian Transport (STILT) model. *Journal of Geophysical Research*, *108*(D16), 4493. https://doi.org/10.1029/2002jd003161

Lu, X., Zhang, X., Li, F., Cochrane, M. A., & Ciren, P. (2021). Detection of fire smoke plumes based on aerosol scattering using VIIRS data over global fire-prone regions. *Remote Sensing*, *13*(2), 1–22. https://doi.org/10.3390/rs13020196

Lutz, J. A., Furniss, T. J., Johnson, D. J., Davies, S. J., Allen, D., Alonso, A., et al. (2018). Global importance of large-diameter trees. *Global Ecology and Biogeography*, *27*(7), 849–864. https://doi.org/10.1111/geb.12747

Luyssaert, S., Knohl, A., Hessenmöller, D., Ciais, P., Law, B. E., Börner, A., et al. (2008). Old-growth forests as global carbon sinks. *Nature*, *455*(7210), 213–215. https://doi.org/10.1038/nature07276

Martin, P. (1989). The significance of radiative coupling between vegetation and the atmosphere. *Agricultural and Forest Meteorology*, *49*(1), 45–53. https://doi.org/10.1016/0168-1923(89)90061-0

Martin, T. A., Hinckley, T. M., Meinzer, F. C., & Sprugel, D. G. (1999). Boundary layer conductance, leaf temperature and transpiration of Abies amabilis branches. *Tree Physiology*, *19*(7), 435–443. https://doi.org/10.1093/treephys/19.7.435

McKendry, I. G., Christen, A., Lee, S. C., Ferrara, M., Strawbridge, K. B., O'Neill, N., & Black, A. (2019). Impacts of an intense wildfire smoke episode on surface radiation, energy and carbon fluxes in southwestern British Columbia, Canada. *Atmospheric Chemistry and Physics*, *19*(2), 835–846. https://doi.org/10.5194/acp-19-835-2019

Meinzer, F. C., Brooks, J. R., Domec, J., Gartner, B. L., Warren, J. M., Woodruff, D. R., et al. (2006). *Dynamics of water transport and storage in conifers studied 105–114*.

Nehrkorn, T., Eluszkiewicz, J., Wofsy, S. C., Lin, J. C., Gerbig, C., Longo, M., & Freitas, S. (2010). Coupled weather research and forecasting-stochastic time-inverted Lagrangian transport (WRF-STILT) model. *Meteorology and Atmospheric Physics*, *107*(1–2), 51–64. https://doi.org/10.1007/s00703-010-0068-x

Norman, J. M., & Becker, F. (1995). Terminology in thermal infrared remote sensing of natural surfaces. *Agricultural and Forest Meteorology*, *77*(3–4), 153–166. https://doi.org/10.1016/0168-1923(95)02259-Z

Novick, K. A., Ficklin, D. L., Stoy, P. C., Williams, C. A., Bohrer, G., Oishi, A. C., et al. (2016). The increasing importance of atmospheric demand for ecosystem water and carbon fluxes. *Nature Climate Change*, *6*(11), 1023–1027. https://doi.org/10.1038/nclimate3114

Oren, R., Sperry, J., Katul, G., Pataki, D., Ewers, B., Phillips, N., & Schäfer, K. (1999). Survey and synthesis of intra-and interspecific variation in stomatal sensitivity to vapour pressure deficit. *Plant, Cell and Environment*, *22*(12), 1515–1526. https://doi.org/10.1046/j.1365-3040.1999.00513.x

Pan, Y., Birdsey, R. A., Fang, J., Houghton, R., Kauppi, P. E., Kurz, W. A., et al. (2011). A large and persistent carbon sink in the world's forests. *Science*, *333*, 988–993.

Park, Y. S., & Paw U, K. T. (2004). Numerical estimations of horizontal advection inside canopies. *Journal of Applied Meteorology*, *43*(10), 1530–1538. https://doi.org/10.1175/jam2152.1

Parks, S. A., Holsinger, L. M., Miller, C., & Parisien, M.-A. (2018). Analog-based fire regime and vegetation shifts in mountainous regions of the western US. *Ecography*, *41*(6), 910–921. https://doi.org/10.1111/ecog.03378

Paw U, K. T., Falk, M., Suchanek, T. H., Ustin, S. L., Chen, J., Park, Y.-S., et al. (2004). Carbon dioxide exchange between an old-growth forest and the atmosphere. *Ecosystems*, *7*(5), 513–524. https://doi.org/10.1007/s10021-004-0141-8

Peltier, D. M. P., & Ogle, K. (2019). Legacies of more frequent drought in ponderosa pine across the western United States. *Global Change Biology*, *25*(11), 3803–3816. https://doi.org/10.1111/gcb.14720

Rastogi, B., Berkelhammer, M., Wharton, S., Whelan, M. E., Itter, M. S., Leen, J. B., et al. (2018). Large uptake of atmospheric OCS observed at a moist old growth forest: Controls and implications for carbon cycle applications. *Journal of Geophysical Research: Biogeosciences*, *123*(11), 3424–3438. https://doi.org/10.1029/2018JG004430

Rastogi, B., Berkelhammer, M., Wharton, S., Whelan, M. E., Meinzer, F. C., Noone, D., & Still, C. J. (2018). Ecosystem fluxes of carbonyl sulfide in an old-growth forest: Temporal dynamics and responses to diffuse radiation and heat waves. *Biogeosciences*, *15*(23), 7127–7139. https://doi.org/10.5194/bg-15-7127-2018

Reichstein, M., Falge, E., Baldocchi, D., Papale, D., Aubinet, M., Berbigier, P., et al. (2005). On the separation of net ecosystem exchange into assimilation and ecosystem respiration: Review and improved algorithm. *Global Change Biology*, *11*(9), 1424–1439. https://doi.org/10.1111/j.1365-2486.2005.001002.x

Roberts, D. A., Ustin, S. L., Ogunjemiyo, S., Greenberg, J., Dobrowski, S. Z., Chen, J., & Hinckley, T. M. (2004). Spectral and structural measures of Northwest forest vegetation at leaf to landscape scales. *Ecosystems*, *7*(5), 545–562. https://doi.org/10.1007/s10021-004-0144-5

Seibt, U., Kesselmeier, J., Sandoval-Soto, L., Kuhn, U., & Berry, J. A. (2010). A kinetic analysis of leaf uptake of COS and its relation to transpiration, photosynthesis and carbon isotope fractionation. *Biogeosciences*, *7*(1), 333–341. https://doi.org/10.5194/bg-7-333-2010

Shaw, D., Franklin, J., Bible, K., Klopatek, J., Freeman, E., Greene, S., & Parker, G. (2004). Ecological setting of the Wind River old-growth forest. *Ecosystems*, *7*(5), 427–439. https://doi.org/10.1007/s10021-004-0135-6

Spielmann, F. M., Wohlfahrt, G., Hammerle, A., Kitz, F., Migliavacca, M., Alberti, G., et al. (2019). Gross primary productivity of four European ecosystems constrained by Joint CO_2 and COS flux measurements. *Geophysical Research Letters*, *46*(10), 5284–5293. https://doi.org/10.1029/2019GL082006

Stephenson, N. L., Das, A. J., Condit, R., Russo, S. E., Baker, P. J., Beckman, N. G., et al. (2014). Rate of tree carbon accumulation increases continuously with tree size. *Nature*, *507*(7490), 90–93. https://doi.org/10.1038/nature12914

Still, C. J., Rastogi, B., Page, G. F. M., Griffith, D. M., Sibley, A., Schulze, M., et al. (2021). Imaging canopy temperature: Shedding (thermal) light on ecosystem processes. *New Phytologist*, *230*(5), 1746–1753. https://doi.org/10.1111/nph.17321

Stimler, K., Berry, J. A., & Yakir, D. (2012). Effects of carbonyl sulfide and carbonic anhydrase on stomatal conductance. *Plant Physiology*, *158*(1), 524–530. https://doi.org/10.1104/pp.111.185926

Strzepek, K., Yohe, G., Neumann, J., & Boehlert, B. (2010). Characterizing changes in drought risk for the United States from climate change. *Environmental Research Letters*, *5*(4), 044012. https://doi.org/10.1088/1748-9326/5/4/044012

Suyker, A., Steiner, A. L., Nadelhoffer, K. J., Phillips, R. P., Hollinger, D. Y., Cheng, S. J., & Bohrer, G. (2014). Variations in the influence of diffuse light on gross primary productivity in temperate ecosystems. *Agricultural and Forest Meteorology*, *201*, 98–110. https://doi.org/10.1016/j.agrformet.2014.11.002

Unsworth, M., Phillips, N., Link, T., Bond, B., Falk, M., Harmon, M., et al. (2004). Components and controls of water flux in an old-growth Douglas fir-Western hemlock ecosystem. *Ecosystems*, *7*(5), 468–481. https://doi.org/10.1007/s10021-004-0138-3

Urban, O., Janouš, D., Acosta, M., Czerný, R., Marková, I., Navrátil, M., et al. (2007). Ecophysiological controls over the net ecosystem exchange of mountain spruce stand. Comparison of the response in direct vs. diffuse solar radiation. *Global Change Biology*, *13*(1), 157–168. https://doi.org/10.1111/j.1365-2486.2006.01265.x

Urban, O., Klem, K., Ač, A., Havránková, K., Holišová, P., Navrátil, M., et al. (2012). Impact of clear and cloudy sky conditions on the vertical distribution of photosynthetic CO_2 uptake within a spruce canopy. *Functional Ecology*, *26*(1), 46–55. https://doi.org/10.1111/j.1365-2435.2011.01934.x

Walker, X. J., Baltzer, J. L., Cumming, S. G., Day, N. J., Ebert, C., Goetz, S., et al. (2019). Increasing wildfires threaten historic carbon sink of boreal forest soils. *Nature*, *572*(7770), 520–523. https://doi.org/10.1038/s41586-019-1474-y

Warren, J., Meinzer, F., Brooks, J., & Domec, J. (2005). Vertical stratification of soil water storage and release dynamics in Pacific Northwest coniferous forests. *Agricultural and Forest Meteorology*, *130*(1–2), 39–58. https://doi.org/10.1016/j.agrformet.2005.01.004

Wehr, R., Commane, R., Munger, J. W., Barry Mcmanus, J., Nelson, D. D., Zahniser, M. S., et al. (2017). Dynamics of canopy stomatal conductance, transpiration, and evaporation in a temperate deciduous forest, validated by carbonyl sulfide uptake. *Biogeosciences*, *14*(2), 389–401. https://doi.org/10.5194/bg-14-389-2017

Wharton, S., & Falk, M. (2016). Climate indices strongly influence old-growth forest carbon exchange. *Environmental Research Letters*, *11*(4), 1–11. https://doi.org/10.1088/1748-9326/11/4/044016

Wharton, S., Schroeder, M., Bible, K., Falk, M., & Paw U, K. T. (2009). Stand-level gas-exchange responses to seasonal drought in very young versus old Douglas-fir forests of the Pacific Northwest, USA. *Tree Physiology*, *29*(8), 959–974. https://doi.org/10.1093/treephys/tpp039

Whelan, M. E., Lennartz, S. T., Gimeno, T. E., Wehr, R., Wohlfahrt, G., Wang, Y., et al. (2018). Reviews and syntheses: Carbonyl sulfide as a multi-scale tracer for carbon and water cycles. *Biogeosciences*, *15*(12), 3625–3657. https://doi.org/10.5194/bg-15-3625-2018

Winner, W., Thomas, S., Berry, J., Bond, B., Cooper, C., Hinckley, T., et al. (2004). Canopy carbon gain and water use: Analysis of old-growth conifers in the Pacific Northwest. *Ecosystems*, *7*(5), 482–497. https://doi.org/10.1007/s10021-004-0139-2

Xu, C., McDowell, N. G., Fisher, R. A., Wei, L., Sevanto, S., Christoffersen, B. O., et al. (2019). Increasing impacts of extreme droughts on vegetation productivity under climate change. *Nature Climate Change*, *9*(12), 948–953. https://doi.org/10.1038/s41558-019-0630-6

Yang, C. E., Hoffman, F. M., Ricciuto, D. M., Tilmes, S., Xia, L., MacMartin, D. G., et al. (2020). Assessing terrestrial biogeochemical feedbacks in a strategically geoengineered climate. *Environmental Research Letters*, *15*(10), 104043. https://doi.org/10.1088/1748-9326/abacf7

Yue, X., & Unger, N. (2018). Fire air pollution reduces global terrestrial productivity. *Nature Communications*, *9*(1), 1–9. https://doi.org/10.1038/s41467-018-07921-4

Zhang, Y., Goll, D., Bastos, A., Balkanski, Y., Boucher, O., Cescatti, A., et al. (2019). Increased global land carbon sink due to aerosol-induced cooling. *Global Biogeochemical Cycles*, *33*(3), 439–457. https://doi.org/10.1029/2018GB006051